Eur Biophys J (2008) 37:411–419
DOI 10.1007/s00249-007-0226-3

ORIGINAL PAPER

Time resolved secretion of chloride from a monolayer of mucin-secreting epithelial cells

Sumitha Nair · Rohit Kashyap · Christian L. Laboisse · Ulrich Hopfer · Miklos Gratzl

Received: 8 February 2007 / Revised: 17 September 2007 / Accepted: 3 October 2007 / Published online: 30 October 2007

Abstract Short-circuit current (Isc) measurement is used to quantify transepithelial ion flux. This technique provides a direct measure of net charge transport across a cell monolayer. Isc however, lacks chemical selectivity. Chemically resolved ion fluxes may be much greater than Isc, and differ in different biological processes. This work describes a novel experimental approach and deconvolution method to obtain temporally resolved ion fluxes at epithelial cell monolayers. HT29-Cl.16E cells, a sub clone of the human colonic cancer cell line HT29 was used as a model cell line to validate this approach in the context of epithelial transport studies. This cell line is known to secrete chloride in response to purinergic stimulation. Changes in chloride concentration after stimulation with 1 mM ATP plus 50 nM phorbol-myristate acetate (PMA) are recorded with a chloride ion-selective electrode (ISE) at a short distance ($\sim$50 μm) from the monolayer. The recorded concentrations are transformed to corresponding chloride flux across the monolayer using a deconvolution algorithm for extracellular mass transport based on minimization of the shape error function (Nair and Gratzl in Anal Chem 77:2875–2888, 2005). Simultaneous voltage clamp yields the associated net electrical charge flux (Isc). The dynamics of Cl^- flux did correlate with that of the electrical flux, but was found to be greater in amplitude. This suggests that Cl^- may not be the only ion secreted. The method of simultaneously assessing ionic and electrical fluxes with a temporal resolution of seconds provides unique information about the dynamics of solute fluxes across the apical membrane.

Electronic supplementary material The online version of this article (doi:10.1007/s00249-007-0226-3) contains supplementary material, which is available to authorized users.

S. Nair · R. Kashyap · M. Gratzl (✉)
Department of Biomedical Engineering,
Case School of Engineering,
Case Western Reserve University,
Cleveland, OH 44106, USA
e-mail: miklos.gratzl@case.edu

C. L. Laboisse
Institut National de la Santé et de la Recherche Médicale 94-04,
Université de Nantes, 44035 Nantes, France

U. Hopfer
Department of Physiology and Biophysics,
School of Medicine, Case Western Reserve University,
Cleveland, OH 44106, USA

Introduction

Short-circuit current (Isc) measurements are often used to quantify net transepithelial ion flux, using ion substitution or isotope flux to infer the nature of the transported ion (Schultz and Leaf 2001). The measured current is a direct indication of physiological transport at the cells' surface. Isc only measures net charge movement and not chemically resolved ion fluxes which may be much greater than Isc and differ in different biological processes. It is therefore desirable to develop methods that resolve the chemical fluxes of ions with a temporal resolution of seconds or better.

One approach is to monitor changes in intracellular ion concentration with fluorescent indicator dyes (Mukonge et al. 2004). The measurements can then be used to compute cellular transport. While this approach works well to characterize the transport properties of membranes, it is poorly suited for epithelia as changes in intracellular ion concentration depend on the sum of apical and basolateral

influx and efflux. Thus under physiological conditions, even large changes in transepithelial fluxes such as in stimulated secretion, might be associated with only small changes in intracellular ion concentrations. Another common approach is the radiotracer flux method (Norez et al. 2004). Here accumulation of transported isotopes in the extracellular trans-compartment is measured. This method suffers from poor temporal resolution and provides unidirectional, but not net, ion fluxes.

Ion-selective electrodes (ISEs) are a better choice to obtain information about ion secretion at high temporal resolution and with good chemical selectivity (Ruzicka 1997). State-of-the art ISEs are selective enough at physiological ion concentrations to differentiate among the different ions that can be secreted. When these sensors are placed in the extracellular space close to a cell layer, they can monitor changes in ion concentrations due to secretion or absorption. The problem that remains is the determination of ion flux at the cell monolayer surface from measurements of concentration changes at some distance.

An existing solution to this problem is offered by the technique of self-referencing electrodes, which is increasingly used for estimating cellular fluxes in both plant (Newman 2001) and animal (Land and Collett 2001; Smith and Trimarchi 2001) cell preparations. Here, the electrode tip is alternately positioned at two distances within the concentration gradient, usually 10 μm apart. The concentration difference between the two points is then used to calculate the corresponding ion flux, assuming a linear concentration profile between the two electrode positions (Newman 2001; Land and Collett 2001; Smith and Trimarchi 2001).

This methodology has limitations in spite of the significant amount of useful data about cellular transport that has been generated with it. The need to avoid excessive mixing around the sensing site restricts the speed of movement of the electrode tip, limiting the temporal resolution to about 0.5 Hz or less. At a cell monolayer the concentration of the secreted solutes varies significantly with distance and rarely in a linear fashion, especially when secretion varies with time (Nair and Gratzl 2005, 2004; Crank 1975; Yi and Gratzl 1998). Moreover, the approach identifies the obtained flux (i.e., flux at some distance from the cells) with flux at the same time at the cell(s). Under conditions when the flux varies nonlinearly with distance this assumption will result in errors that are hard to correct for.

Stationary ISEs provide an alternative to self-referencing electrodes if the problem of back calculation from measured concentration changes to flux at the cells can be solved. Measured concentration changes result from convolution of secretory (or absorptive) solute flux at the cells' surface and mass transport (diffusion) between the surface of the monolayer and the ion sensing electrode (Nair and Gratzl 2005). Thus, calculating flux from concentrations is a deconvolution problem. Proper deconvolution can handle time delay between initiation and sensing of a process and avoids the need to assume a linear decay (or increase) in concentration versus distance. The use of stationary ISEs also avoids the problem of solution mixing.

The nature of mass transport from the cells to the sensor needs to be taken into consideration when estimating fluxes from monitored concentration (Yi and Gratzl 1998; Lu and Gratzl 1999). Diffusion patterns at a distance of about two cell diameters or more above a confluent cell monolayer are comparable with those from an equivalent single planar source. If a sensor is placed no closer than this distance then mass transport from the cells to the sensor can be assumed to be essentially planar. Planar or one dimensional diffusion is, however, inefficient and results in a time lag between events of cellular transport and their detection at the sensor (Crank 1975). Thus, it can only be represented as a convolution integral (Nair and Gratzl 2005) as opposed to an algebraic equation. Therefore, to infer ion flux from the measured concentration time series, it is necessary to solve the complete deconvolution problem, rather than rely on a simple (e.g., linear) approximation. A novel deconvolution method that uses the concept of "function shape" has been developed by two of the authors (Nair and Gratzl 2005). The shape based deconvolution algorithm has been successfully used to determine dynamics of doxorubicin efflux from doxorubicin concentration changes measured (with a carbon fiber electrode) close to monolayers of multidrug resistant and drug sensitive cancer cells (Nair and Gratzl 2004, 2005).

In this study, the problem of assessing secretory ionic fluxes from an epithelial monolayer with high temporal resolution is addressed with ISEs and the shape based deconvolution algorithm. The ISE is placed at a distance $\sim$50 μm above the monolayer surface and monitors ion concentration as a function of time in response to stimulated secretion. The deconvolution procedure converts these data to dynamic ion fluxes at the cells. At the same time, the net charge flux across the epithelium is measured directly as Isc with a voltage clamp. This makes it possible to compare net charge flux with net ion flux.

The result of such comparison is not trivial if more than one ion is involved in electrolyte secretion since then the amplitude and time course of the Isc will represent only the sum total of individual ionic fluxes. Suitable ISEs can, however, indicate transport of different individual ions. Combined Isc and ISE recordings thus provide more than just one lumped piece of information about the same biological process. Eventual discrepancies would be indicative of transport of multiple electrolytes. Moreover, transport of ions through electrically silent pathways such as release of

vesicular content will not be measured by Isc but is accessible to ISEs. To increase sensitivity of the ISE measurement, however, it is desirable to decrease the background concentration of the ion that is measured in the apical compartment. This asymmetry in concentration could result in some passive basal to apical flux of the studied ion through the tight junction. Based on experimental results and theoretical considerations such parasitic transport was found, however, negligible in this work, as discussed later. The proposed approach that enables simultaneous recording of Isc and ISE therefore could open up new avenues for a more comprehensive study of epithelial secretion processes.

HT29-Cl.16E was used as a model epithelium to validate the relevance of this approach to transepithelial transport studies. Cl.16E is a clone of the human colonic cancer cell line HT29. It forms relatively well-differentiated mucin and electrolyte secreting monolayers. Previous work (Merlin et al. 1994) established that several types of secretagogues stimulate mucin and Cl^- secretion from these cells, purinergic stimulation with apical ATP being most effective. The experimental and mathematical tools described in this work have made it possible to study temporally resolved Cl^- secretion concurrent with net charge transport.

Materials and methods

Materials

Dulbecco's modified eagle's medium (DMEM), Ham's F12 and fetal bovine serum (FBS) were bought from GIBCO (Grand Island, NY, USA). Vitrogen is a product of Celtrix Lab (Palo Alto, CA, USA). Adenosine triphosphate (ATP), Phorbol-12-myristate-13-acetate (PMA) and all other chemicals were bought from Sigma-Aldrich (St. Louis, MO, USA).

Cell culture

HT29-C1.16E cells were propagated in Falcon culture flasks (25 cm^2) in a humidified atmosphere of 95% air and 5% CO_2 at 37°C. The cells were fed every day with DMEM supplemented with 10% heat inactivated FBS and 4 mM L-glutamine. The passage numbers for the reported experiments are between 30 and 47. For electrophysiological and ion-selective electrode (ISE) measurements, the cells were grown on Vitrogen coated Millicell-CM filter (Millipore, Bedford, MA, USA, 10 mm). The cells were seeded at a density of 1.2×10^6/filter (area: 0.6 cm^2). The cells became visually confluent after 1 week and were used for secretion studies 12–18 days after seeding. All monolayers had resistances of at least 250 Ω cm^2.

Electrophysiology

Transepithelial electrophysiological measurements were carried out in an Ussing type chamber (Analytical Bioinstrumentation, Cleveland, OH, USA) constructed to accept Millicell-CM filters. The chamber was modified to accept four electrodes (two apical and two basal electrodes) for the voltage clamp (Model 558-C-5, Bioengineering Department, University of Iowa, Iowa City, IA, USA) and two for an ISE cell in the apical compartment. The schematic of the experimental setup is shown in Fig. 1. The chamber was grounded through the voltage clamp. The transepithelial potential was clamped to zero and the Isc was obtained. The ISE reference was independent of the one used for voltage clamp circuit. The current output from the clamp and the voltage of the ISE were digitized and stored in a computer. Positive currents correspond to anion secretion/cation absorption. Before each experiment the voltage output of the clamp was adjusted to zero to compensate for any asymmetry in the voltage-sensing electrodes, and fluid resistance was compensated using a blank Millicell-CM filter. The chamber and all solutions were maintained at 37°C in a Plexiglas incubator during the experiments.

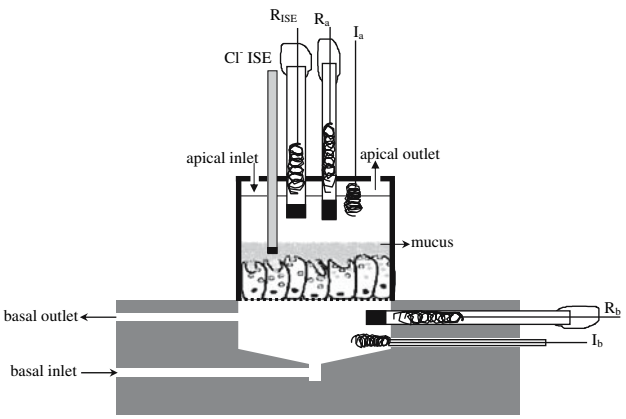

Fig. 1 Experimental setup for simultaneous measurements of Isc and temporally resolved concentration changes of Cl^- with ISE in an Ussing chamber. A standard four-electrode setup is used for voltage clamp: I_a and I_b are current passing platinum electrodes, and R_a and R_b are Ag/AgCl electrodes with liquid junctions on the apical or basal side. *ISE* refers to ion-selective electrode for Cl^- in the apical compartment. A separate reference electrode R_{ISE} is used for the ISE measurement to avoid cross talk with voltage clamp measurement. The basal chamber is continuously perfused to provide oxygen, while apical perfusion is completely stopped during experiments

Experimental protocol

A filter covered with a monolayer of cells was placed in the chamber. The basal side was perfused with HEPES buffered normal Ringer solution (114 mM NaCl, 4 mM KCl, 1.25 mM $CaCl_2$, 1 mM $MgCl_2$, 10 mM HEPES, 5.6 mM glucose). The solution for the apical chamber was a low Cl^- HEPES buffered Ringer solution s14 mM Na^+-gluconate, 200 μM KCl, 60 μM $CaCl_2$, 1 mM $MgCl_2$, 10 mM HEPES, 5.6 mM glucose). The pH of the apical and basal solution was adjusted between 7.2 and 7.4 using NaOH. The ISEs were placed ~50 μm above the cell surface, using an AC impedance technique (Kashyap and Gratzl 1999). To initiate secretion of mucin and electrolytes, 1 mM ATP + 50 nM PMA was added to the apical chamber. Data were collected starting shortly before addition of secretagogue and lasted for another 9–10 min after addition. The apical chamber perfusion was stopped during the measurements. In the set of monolayers used in this study, the inclusion of 50 nM PMA in the ATP solution increased the Isc response, presumably by increasing the sensitivity of cells to purinergic stimulation. Fifty nano molar PMA by itself had no effect on the Isc.

Ion selective electrodes

Chloride electrode

The Cl^- electrode used in this work consists of a silver wire with Teflon insulation (OD ≈ 250 μm). One end of the Teflon coated silver wire was chloridized to get a Ag|AgCl interface which is the sensing element. The potential arising at the Ag|AgCl interface was proportional to the logarithm of concentration of Cl^- ions in the buffer solution. The other end of the silver wire was stripped and connected to a gold pin to be hooked up to an amplifier. The calibration curve for the Cl^- electrode in low Cl^- Ringer solution was obtained and the data was least squares fit with the Nicholsky–Eisenman equation (Morf 1981). The electrode has a close to theoretical (61 mV/decade) sensitivity of 60.3 ± 0.5 mV/decade (n = 5) at 37°C and the response was log-linear from 10^{-4} to 10^{-1} M. The response time (90% change in potential) of this electrode is less than 1 s. It can therefore be used to detect changes happening on the order of a few seconds while Cl^- secretion occurs on the minutes scale. The electrodes were found to be stable over a period of 2 h with a mean potential drift of less than 1 mV/h.

Reference electrodes for voltage clamp and ISE measurements

The electrode body was made of 18 gauge shrink teflon tubing (Small Parts Inc., Miami Lakes, FL, USA). One end of the tubing was sealed with a ceramic plug. A small ceramic plug (2 mm in length) was first inserted into a Pyrex disposable micro pipette (Corning, NY, USA). The micro pipette was heated and pulled over a glass flame so that it seals the ceramic plug tightly. The micro pipette was then cut on both sides of the ceramic plug using a diamond glass cutter. On one end the ceramic plug was almost flush with the glass whereas on the other end about 5–7 mm of glass was left. The flush end was then polished mechanically. The extended end of the glass piece containing the ceramic plug was then inserted into the shrink teflon tubing. The tubing was sealed onto the glass over a heated soldering iron. The electrode body is back filled with internal filling solution making sure that no bubbles were trapped at the edge of the glass and teflon tubing. A Ag|AgCl (d ≈ 1 mm) wire was inserted into the electrode and parafilm was used to seal the electrode body and the wire together.

Back calculation of secretion flux from measured concentration data

Secretion of Cl^- was quantified from the respective concentrations measured at ~50 μm from the epithelial cell monolayer using a novel deconvolution algorithm based on function shape (Nair and Gratzl 2005). The optimization was performed using Matlab (The Mathworks, Natick, MA, USA) 7.0.4, Release 14. Briefly, concentration dynamics at the sensor's distance was predicted using the convolution integral for planar diffusion (Nair and Gratzl 2004) for an initial assumption of constant flux. "Distance" between the measured concentration trace and the estimated one is then minimized. This distance is defined as the difference in "shape" between the measured and predicted concentration time series. Function shape is defined as the direction of a vector of N concentration data in an N dimensional space. The individual vector components represent concentration values measured at regular time intervals (e.g. 1 s in this case). Thus, shape error is the "angle" between the measured and estimated concentration dynamics as given by Eq. (1) (Nair and Gratzl 2005) where C refers to vectors of time series concentration data.

$$\text{Shape error} = \arccos\left[\mathbf{C}_{\text{estimated}}\mathbf{C}_{\text{measured}}/|\mathbf{C}_{\text{estimated}}|\,|\mathbf{C}_{\text{measured}}|\right]. \quad (1)$$

Minimization of shape error renders the shape of the measured and estimated concentration traces similar: a procedure equivalent to deconvolution. The corresponding secretion dynamics is then expected to be also similar to the actual physiological transport that induced the

measured data. Shape optimization was found more efficient than other techniques in solving deconvolution in the context of cellular transport studies (Nair and Gratzl 2005). The flow diagram for the optimization is provided in supplement 1.

Equation (1) is essentially the inverse of the dot product (Stewart 2002) of two vectors. To further understand the concept of shape let us consider an example wherein the stimulation dependent concentration change that is measured, $\mathbf{C}_{measured}$, corresponds to 0 concentration at time $t = 0$ and by time $t = 10$ min the concentration increases to 1. This concentration "dynamics" can be represented as a vector in a two dimensional space, with the x axis being the concentration value at $t = 0$ and the y axis being the concentration value at $t = 10$ min. This vector makes an angle of 90° with the x axis.

Now let us assume that the concentration corresponding to the initial assumption of flux density, $\mathbf{C}_{estimated}$ has a constant value, e.g., 1 at times $t = 0$ and 10 min. This vector makes an angle of 45° with the x axis. The angle difference between $\mathbf{C}_{estimated}$ and $\mathbf{C}_{measured}$ based on Eq. (1) is 45° for this very simple example; the same can be obtained graphically. The angle difference of 45° indicates that these two vectors do not have the same orientation in the two dimensional space and are therefore not identical in shape. What the optimization does is to change the flux such that the angle difference between $\mathbf{C}_{estimated}$ and $\mathbf{C}_{measured}$ decreases with each iteration. In other words by the end of the optimization the vector represented by $\mathbf{C}_{estimated}$ will be oriented such that it will make an angle of nearly 0° with the vector of measured concentrations, or ~90° with the x axis. The corresponding flux indicates the physiological transport at the cells that resulted in $\mathbf{C}_{measured}$.

Results

HT29-Cl.16E cells are known to secrete Cl^- when stimulated by luminal ATP (Merlin et al. 1994). In this work a Cl^- ISE was employed for correlating chemically resolved Cl^- ionic flux density with simultaneously measured electrical current density (Isc). The experimental arrangement is shown in Fig. 1. Addition of ATP + PMA to the apical compartment caused an almost immediate decrease in the potential measured by the Cl^- ISE positioned ~50 µm from the cell monolayer. This decrease in potential corresponds to an increase in Cl^- concentration that was sustained over the entire ~10 min duration of the measurement. The maximum potential change was 29.5 ± 3.6 mV (n = 10). This corresponds to an increase in concentration of 4.8 ± 0.7 mM over the baseline. The recorded concentration (Fig. 2a, solid line) was translated to Cl^- flux density at the cells (Fig. 2b) using shape optimization (see "Materials and methods"). The flux density is indicated in both chemical (left ordinate) and equivalent electrical (right ordinate) units to

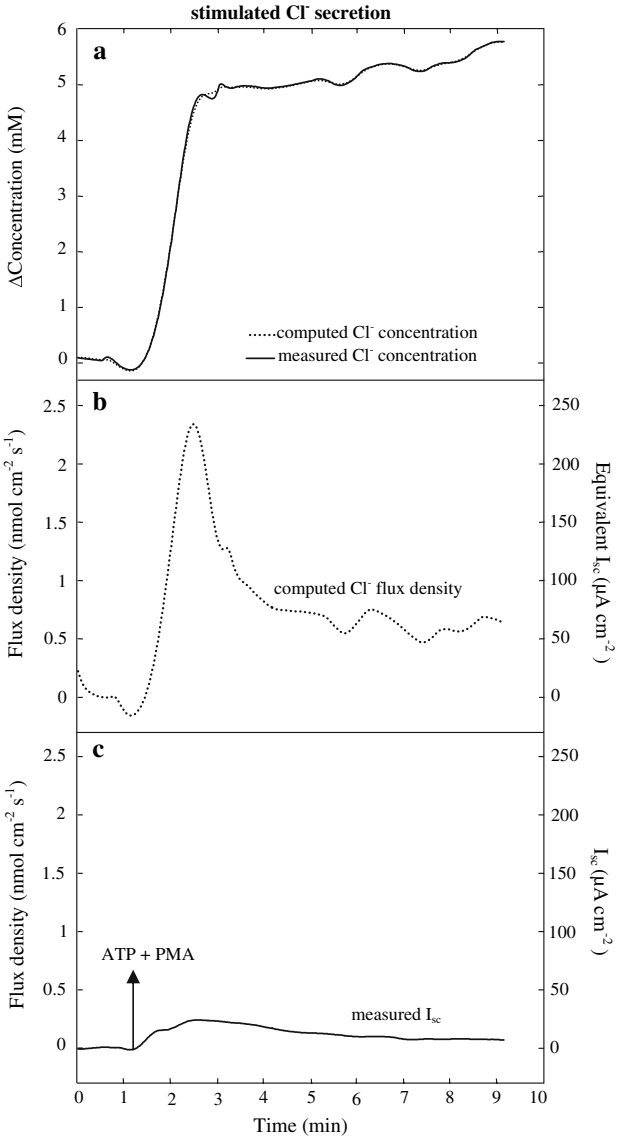

Fig. 2 Time courses of ion concentration, flux and Isc in response to stimulation of HT29-Cl.16E monolayer. Data were collected for ~1.5 min at which time mucin and electrolyte secretion was initiated by addition of apical ATP (1 mM) plus PMA (50 nM). **a** Concentration traces; measured *solid line*, computed *dotted line*. **b** Computed ion flux density in electrical (*right axis*) and equivalent molar units (*left axis*). **c** Simultaneously measured Isc expressed in electrical (*right axis*) and equivalent molar units corresponding to secretion of a univalent ion (*left axis*). The Cl^- flux density was computed from the measured concentration shown in **a** using shape optimization as described in the "Materials and methods". The diffusion coefficient of Cl^- used for the optimization was adjusted for mucus, as reported (Guth and von Engelhardt 1989). For the optimization electrode distance from the monolayer was assumed to be 50µm

facilitate comparison with the measured electrical flux (Fig. 2c).

As shown in Fig. 2c addition of ATP + PMA to the apical compartment resulted in an immediate increase in Isc that implies a secretory anion current (or absorptive cation current). The Isc reached its peak within the next ~2 min and then began to slowly decline towards baseline. Earlier studies have shown that Cl^- secretion from these cells is a major constituent of the measured Isc (Merlin et al 1994). Chloride is secreted through Cl^- channels located in the plasma membrane and those derived from recruitment of Cl^- channels located in the granule membrane (Merlin et al. 1996). The measured Isc is also represented in chemical units (Fig. 2c, left ordinate) corresponding to equivalent secretion of a univalent anion. These results are from a representative experiment of a total of ten parallels each using a separate filter.

The dotted lines in Fig. 2a represent concentration dynamics that correspond to the computed Cl^- flux density shown in Fig. 2b. The error in shape expressed in angle between the shape vector of concentration corresponding theoretically to the back calculated flux density and that of the shape vector of measured concentration is less than 0.7°. This is an indication that the optimization converged to a flux density that fits the overall trend in measured concentration. A perfect fit in shape would produce an error of 0° (Nair and Gratzl 2005).

Discussion

The objective of the reported experiments and mathematical method is to reconstruct the dynamics of stimulated Cl^- secretion in HT29-Cl.16E cells and to correlate it with the measured Isc. Temporally resolved Cl^- flux was obtained from the concentrations measured by a Cl^- ISE positioned at a fixed distance from the monolayer using an algorithm based on function shape. ISEs are known for reproducibly monitoring concentration changes in buffers containing biological specimens (Koryta 1986). The optimization itself reproducibly converges to a flux that corresponds to a concentration that is closest in shape to the measured concentration trace. Diffusion constant of Cl^- and distance of electrode from the cells are parameters that are used for the optimization. The effect of uncertainty in these parameters on the flux calculated with shape optimization is discussed below. In addition the effect of asymmetric Cl^- concentration on the measurement is also explained. A comparison of the chemical flux with the charge flux is provided and physiological relevance of the approach is also addressed.

Table 1 Effect of a hypothetical variability in diffusion constant on Cl^- flux density back calculated with shape optimization

Diffusion constant ($cm^2\ s^{-1}$)	Peak of back calculated Cl^- flux density (nmol $cm^2\ s^{-1}$)
$1.11 \times 10^{-5}(0.93 \times 10^{-5} + 20\%)$	2.44
0.93×10^{-5} (adjusted for mucus)	2.22
$0.74 \times 10^{-5}(0.93 \times 10^{-5} - 20\%)$	2.07

The electrode distance from the monolayer was assumed to be 50 μm

Effect of variability in diffusion constant on the estimated flux

Our data interpretation assumes that the ISE is immersed in the mucus layer during the course of measurements. The diffusion constant for Cl^- in water was therefore adjusted for the more viscous mucus. Based on reported results (Guth and von Engelhardt 1989) a value of 0.93×10^{-5} $cm^2\ s^{-1}$ (54% lower than in water) was used as the diffusion constant of Cl^- in the optimization. The effect of a hypothetical ±20% uncertainty in Cl^- diffusion constant, an error that is likely much higher than any realistic error in the reported value (Guth and von Engelhardt 1989), on the estimated Cl^- flux was evaluated; the results are summarized in Table 1. The peak of the estimated Cl^- flux shows ~5% variation for a 10% relative variability in diffusion constant. Thus the optimization is not very sensitive to error in diffusion constant.

Effect of electrode placement on the estimated flux

In this study, diffusion of the secreted Cl^- away from the cell monolayer is assumed to be planar or one-dimensional in nature. This is valid if the sensor is placed far enough where the diffusion profiles from the individual cells largely overlap (Nair and Gratzl 2005). The diameter of HT29-Cl.16E cells is ~8–15 μm. Placing the sensor at a distance of 50 μm, as in the reported experiments, therefore satisfies this condition. It was experimentally verified that the Cl^- electrode could be reproducibly positioned up to 250 μm from a planar surface or from a cell monolayer with a precision of ±5 μm (Kashyap and Gratzl 1999). The effect of hypothetical uncertainties in electrode positioning on the calculated flux was evaluated by varying the ISE distance from the surface in the deconvolution calculations; the results are summarized in Table 2. The peak of the estimated Cl^- flux shows a variation <1% for a 10% relative variability in electrode positioning. This means that error in electrode placement has very little affect on the estimated flux.

Table 2 Effect of a hypothetical variability in distance on Cl^- flux density back calculated with shape optimization

Distance (μm)	Peak of back calculated Cl^- flux density (nmol cm^2 s^{-1})
45	2.24
50	2.22
55	2.25

The Cl^- diffusion constant was assumed to be 0.93×10^{-5} cm^2 s^{-1}

Potential effect of asymmetric chloride concentration on the measurement

As normal HEPES-buffered Ringer solution was present on the basal side of the monolayer and low Cl^- HEPES-buffered Ringer solution on the apical side, asymmetric Cl^- concentrations existed on the two sides of the monolayer. This could theoretically produce a diffusional basal-to-apical flux of Cl^-. Several observations argue that the possibility of net paracellular transport of Cl^- is minor and would not alter the interpretation of the experimental results. (1) There was minimal net movement of Cl^- in the absence of ATP as seen from the relatively flat baselines in ISE and Isc data. This is an indication that the paracellular pathways in the monolayer are relatively impermeable to Cl^- under baseline conditions. (2) All monolayers used were intact as assessed by electrical resistance. ATP stimulation of these cells produces an increase in DC resistance the time course of which mirrors that of the Isc (Bertrand et al. 1999). Hence, any hypothetical ion flux through the paracellular pathways would be least when the measured Isc is maximum, minimizing an eventual distorting effect in the region of greatest interest. (3) The time course and peak of Isc measured in response to ATP stimulation in our experiments is comparable with published results that have been obtained under symmetric ion concentrations (Merlin et al. 1994, 1996; Bertrand et al. 1999). This indicates that the current measured under asymmetric condition predominantly reflects transcellular transport. (4) In this work the maximum possible flux of Cl^- through the paracellular pathway was also modeled and compared to the measured flux (Fig. 3).

The model is based on Fick's diffusion equation and the assumptions that (1) the diffusion constant of Cl^- in the paracellular space is same as in water and (2) the measured electrical conductance of the monolayer is completely due to Cl^- permeability through tight junctions (for derivation of equations see supplement 2). Time dependant resistance of the monolayer during ATP stimulation obtained from prior published results (Bertrand et al. 1999; Fig. 1b) was also incorporated into the model. The theoretically predicted response of the ISE to diffusional transport through paracellular pathways and the measured response is shown in Fig. 3. The differences during both the baseline and stimulated period suggest that, even in worst case scenario, paracellular net movement of Cl^- cannot explain the measured electrolyte flux during stimulation. Thus paracellular flux of Cl^- must be very low, if any. These considerations suggest that the Cl^- flux computed from ISE measurements is essentially the result of transcellular Cl^- transport. Hence the asymmetric Cl^- concentration did not distort the electrolyte secretion process.

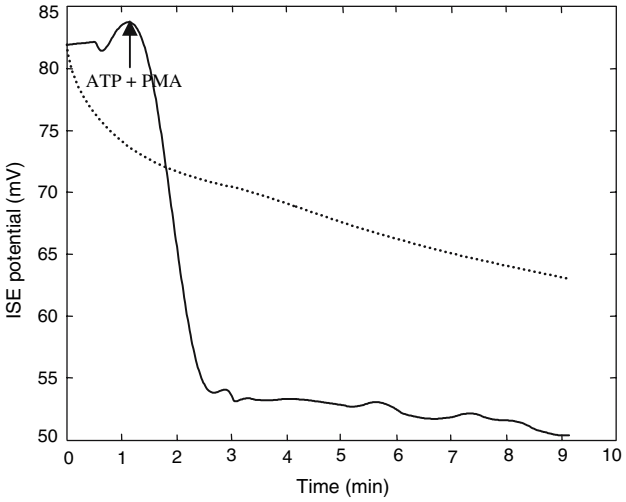

Fig. 3 The Cl^- ISE recording in response to apical stimulation is compared with the expected response to diffusional flux through the paracellular pathways. The response of the ISE to transport through the tight junction is calculated using Eq. (5) in supplement 2 and experimental data (Bertrand et al. 1999; Fig 1b) reported on time dependant monolayer resistance, including during stimulation, of the monolayer. *Solid line* measured response of the ISE to apical stimulation. *Dotted line* theoretically expected response of the ISE to diffusional transport through paracellular pathways for diffusion constant (D) of Cl^- as in water:$D_{Cl^-} = 2.03 \times 10^{-5}$ cm^2 s^{-1}

Comparison between chemical flux and charge flux

The Isc measured in this work is similar to that measured previously (Merlin et al. 1994, 1996) and is explained by transport through Cl^- channels in the luminal plasma membrane and those recruited from the granule membrane. The Cl^- flux density obtained in this work did correlate temporally with the Isc, but was greater in magnitude. The peak of Cl^- flux density was unexpectedly high, approximately ten times the peak of simultaneous electrical charge flux. To test whether this discrepancy is a result of potential uncertainty in reported diffusion constant and/or electrode distance used in the optimization, the back calculated flux was validated using first principles.

The total amount of ions that would have moved to the apical compartment during an experiment may be estimated

by mixing the apical compartment at the end of the experiment and measuring its volume and the concentration of the ion of interest with an ISE. The product gives the net change in ion content during the experiment. The total amount of Cl^- secreted can also be obtained from the integral of the flux shown in Fig. 2b. This was found to be 0.24 μmol while that from the ISE measurement at the end of the experiment after stirring of the apical compartment is 0.27 ± 0.04 μmol ($n = 10$). There is a remarkably good agreement between the total cumulative Cl^- efflux computed from continuous recording of Cl^- concentrations, and from physical measurement of total Cl^- released by the end of the experiment. This holds for all ten parallel experiments. This observation corroborates that the higher than expected amplitude of the Cl^- flux found is not a result of the potential errors in the measurement scheme and uncertainties in diffusion constant of Cl^- and electrode placement. This is also indicative of the robustness of the approach since an estimate of the total amount of Cl^- movement from the basal to apical side must reflect the cumulative uncertainty of the entire scheme including those in the ISE measurement, diffusion constant and electrode positioning.

The Isc corresponds to secretion of a total of 0.04 ± 0.01 μmol ($n = 10$) of univalent ion. This infers that the Isc alone is not indicative of the total Cl^- secretion and that in the mucin secreting HT29-Cl.16E cell line, Cl^- may not be the only ion secreted. Simultaneous cation secretion or anion absorption would lead to a decrease in Isc relative to that which is comprised of Cl^- flux alone. Another possibility is may be the presence of electrically silent pathways for Cl^- secretion.

Physiological relevance of the combined Isc and ISE measurement scheme

The adaptation of stationary ISEs for measurement of chemical flux in proximity of biological specimens can improve sensitivity and temporal resolution of the experimental approach. Previous studies to obtain chemically resolved ion fluxes relied either on removing aliquots of the solution and measuring their ion contents at subsequent time points or calculating net flux from two unidirectional isotope fluxes. These methods have low sensitivity and temporal resolution. Yet as seen in the experiments reported here, the changes in electrical and chemical fluxes occur within a time frame of 2–5 min. Dynamics occurring on this time scale can be resolved only by placing a suitable probe such as an ISE close enough to the source so that temporal changes in ion fluxes can lead to discernable ion concentration changes at the distance of the sensor.

Earlier studies had established that extracellular ATP elicits simultaneous mucus and electrolyte release from HT29-Cl.16E cells (Merlin et al. 1994), using electrical flux (Isc) as surrogate for electrolyte secretion. Those earlier experiments are complemented by the ones discussed in this work with a possible new interpretation of some results. An interesting observation in the earlier experiments (Merlin et al. 1994) was that replacement of Cl^- by gluconate in the basal perfusion with a preincubation of 60 min did not completely abolish the Isc elicited by a purinergic agonist (ATP), in contrast to those stimulated by cAMP or a cholinergic agonist (carbachol). Of the ATP-stimulated Isc only 40% of the peak Isc and 80% of the total charge movement (integrated Isc) was "Cl^- sensitive". These observations were interpreted in terms of the classical Cl^- secretion model (Silva et al. 1977), whereby the lack of complete Cl^- sensitivity of Isc with purinergic stimulation was explained by insufficient depletion of intracellular Cl^- during the preincubation period. The present finding that the Isc represents just a fraction of the stimulated Cl^- secretion in HT29-Cl.16E cells indicates the ambiguity in interpretation of Isc data in terms of the underlying electrolyte fluxes. Future experiments with ISEs for other ions, e.g., Na^+, K^+ and H^+ will provide a more comprehensive picture of purinergically stimulated electrolyte secretion in Cl.16E cells.

Conclusions

The experimental and mathematical approach discussed in this work has made it possible to dynamically monitor purinergically stimulated Cl^- secretion from HT29-Cl.16E cells. The results from this study demonstrate the validity of using stationary ISEs in conjunction with conventional epithelial electrophysiology. The ISE measurements provide chemically resolved fluxes. Such measurements can also be performed in the absence of voltage clamp. Thus providing greater insight into physiologically possible ion flux rather than just the maximal transport capacity of the monolayer measured under short-circuit condition. Low background concentration of the ion of interest may improve sensitivity of the measurements. The use of ion selective electrodes together with short circuit current measurements makes two pieces of information about the biological transport of interest available: chemically resolved flux densities and net charge transport. These data are complementary and enable cross-verification of results. This is especially useful in cases when the net electrical flux might be the result of transport of more than one ion. Thus additional information about individual chemical fluxes can provide a more comprehensive picture of transepithelial transport processes as well as aid in designing future studies.

Acknowledgments We thank Dr. Calvin U. Cotton for helpful discussions during the preparation of this manuscript. The authors thank Mabintou Traore for performing early feasibility studies. This work was supported by funds from the National Institute of Health (Grant CA-61860 to MG), the Cystic Fibrosis Foundation (Grants HOPFER99PO to UH and G813 to MG) and Ohio Board of Regents Innovation Incentive Fellowship award to Sumitha Nair.

References

Bertrand CA, Laboisse CL, Hopfer U (1999) Purinergic and cholinergic agonists induce exocytosis from the same granule pool in HT29-Cl.16E monolayers. Am J Physiol Cell Physiol 276 (45):C907–C914

Crank J (1975) The mathematics of diffusion, 2nd edn. Clarendon Press, Oxford

Guth D, von Engelhardt W (1989) Is gastro-intestinal mucus an ion-selective barrier? Symp Soc Exp Biol 43:117–121

Kashyap R, Gratzl M (1999) Adjusting the distance of electrochemical microsensors from secreting cell monolayers on the micrometer scale using impedance. Anal Chem 71:2814–2820

Koryta J (1986) Ion-selective electrodes. Ann Rev Mater Sci 16:13–27

Land SC, Collett A (2001) Detection of Cl^- flux in the apical microenvironment of cultured foetal distal lung epithelial cells. J Exp Biol 204:785–795

Lu HW, Gratzl M (1999) Monitoring drug efflux from sensitive and multidrug-resistant single cancer cells with microvoltammetry. Anal Chem 71:2821–2830

Merlin D, Augeron C, Tien XY, Guo X, Laboisse CL, Hopfer U (1994) ATP-stimulated electrolyte and mucin secretion in the human intestinal goblet cell line HT29-Cl.16E. J Membr Physiol 137:137–149

Merlin D, Guo X, Martin K, Laboisse CL, Landis D, Dubyak G, Hopfer U (1996) Recruitment of purinergically stimulated Cl^- channels from granule membrane to plasma membrane. Am J Physiol Cell Physiol 271(40):C612–C619

Morf WE (1981) The principles of ion-selective electrodes and of membrane transport, 1st edn. Elsevier, Amsterdam

Mukonge F, Alton EW, Andersson C, Davidson H, Dragomir A, Edelman A, Farley R, Hjelte L, McLachlan G, Stern M, Roomans GM (2004) Measurement of halide efflux from cultured and primary airway epithelial cells using fluorescence indicators. J Cyst Fibros 3:171–176

Nair S, Gratzl M (2004) Anomalies of deconvolution via discrete Fourier transform: a case study on assessing transport at live cell preparations. Trends Anal Chem 23:459–467

Nair S, Gratzl M (2005) Deconvolution of concentration recordings at live cell preparations via shape error optimization. Anal Chem 77:2875–2888

Newman IA (2001) Ion transport in roots: measurement of fluxes using ion-selective microelectrodes to characterise transporter function. Plant Cell Environ 24:1–14

Norez C, Heda GD, Jensen T, Kogan I, Hughes LK, Auzanneau C, Derand R, Bulteau-Pignoux L, Li C, Ramjeesingh M, Li H, Sheppard DN, Bear CE, Riordan JR, Becq F (2004) Determination of CFTR chloride channel activity and pharmacology using radiotracer flux methods. J Cyst Fibros 3:119–121

Ruzicka J (1997) The seventies—Golden age for ion selective electrodes. J Chem Ed 74:167–170

Schultz SG, Leaf A (2001) Hans Ussing memorial issue: epithelial membrane transport. J Membr Biol 184:199–202

Silva P, Stoff J, Field M, Fine L, Forrest JN, Epstein FH (1977) Mechanism of active chloride secretion by shark rectal gland: role of Na–K–ATPase in chloride transport. Am J Physiol 233:F298–F306

Smith PJS, Trimarchi J (2001) Noninvasive measurement of hydrogen and potassium ion flux from single and epithelial structures. Am J Physiol Cell Physiol 280:C1–C11

Stewart J (2002) Calculus, 5th edn. Brooks Cole, California

Yi C, Gratzl M (1998) Continuous in situ electrochemical monitoring of doxorubicin efflux from sensitive and drug-resistant cancer cells. Biophys J 75:2255–2261